



**HAL**  
open science

## Magnetotactic bacteria as a new model for P sequestration in the ferruginous Lake Pavin

S. Rivas-Lamelo, K. Benzerara, C. T Lefèvre, C. L Monteil, D. Jézéquel, N. Menguy, E. Viollier, F. Guyot, C. Féraud, M. Poinsot, et al.

### ► To cite this version:

S. Rivas-Lamelo, K. Benzerara, C. T Lefèvre, C. L Monteil, D. Jézéquel, et al.. Magnetotactic bacteria as a new model for P sequestration in the ferruginous Lake Pavin. *Geochemical Perspectives Letters*, 2017, 5, pp.35-41. 10.7185/geochemlet.1743 . hal-01741645

**HAL Id: hal-01741645**

**<https://hal.sorbonne-universite.fr/hal-01741645>**

Submitted on 23 Mar 2018

**HAL** is a multi-disciplinary open access archive for the deposit and dissemination of scientific research documents, whether they are published or not. The documents may come from teaching and research institutions in France or abroad, or from public or private research centers.

L'archive ouverte pluridisciplinaire **HAL**, est destinée au dépôt et à la diffusion de documents scientifiques de niveau recherche, publiés ou non, émanant des établissements d'enseignement et de recherche français ou étrangers, des laboratoires publics ou privés.

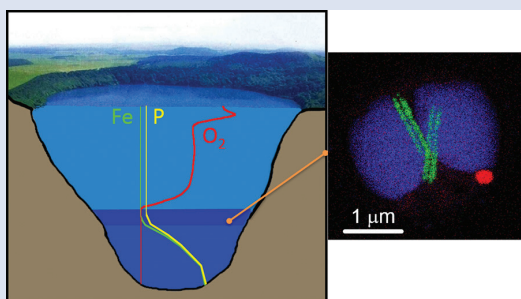
## Magnetotactic bacteria as a new model for P sequestration in the ferruginous Lake Pavin

S. Rivas-Lamelo<sup>1</sup>, K. Benzerara<sup>1\*</sup>, C.T. Lefèvre<sup>2</sup>, C.L. Monteil<sup>2</sup>,  
D. Jézéquel<sup>3</sup>, N. Menguy<sup>1</sup>, E. Viollier<sup>3</sup>, F. Guyot<sup>1</sup>, C. Férard<sup>1</sup>, M. Poinso<sup>1</sup>,  
F. Skouri-Panet<sup>1</sup>, N. Trcera<sup>4</sup>, J. Miot<sup>1</sup>, E. Duprat<sup>1</sup>



doi: 10.7185/geochemlet.1743

### Abstract



The role of microorganisms in the geochemical cycle of P has received great interest in the context of enhanced biological phosphorus removal and phosphorite formation. Here, we combine scanning and transmission electron microscopies, confocal laser scanning microscopy and synchrotron-based x-ray microfluorescence to analyse the distribution of P at the oxic-anoxic interface in the water column of the ferruginous Lake Pavin. We show that magnetotactic bacteria of the *Magnetococcales* family strongly accumulate polyphosphates and appear as P hotspots in the particulate fraction at this depth. This high accumulation may be characteristic of this family and may also relate to the chemical conditions prevailing in the lake. As a result, these magneto-

tactic cocci can be considered as new models playing a potentially important role in the P geochemical cycle, similar to sulphide oxidising bacteria such as *Thiomargarita* and *Beggiatoa* but thriving in a ferruginous, poorly sulphidic environment.

Received 2 June 2017 | Accepted 10 October 2017 | Published 15 November 2017

### Introduction

Magnetotactic bacteria (MTB) are a phylogenetically and metabolically diverse group of bacteria biomineralising intracellular magnetites and/or greigites and moving along magnetic field lines. Since their discovery (Blakemore, 1975), they have been found in various environments worldwide including sediments and the water column of freshwater, marine and hypersaline habitats (Lefèvre and Bazylinski, 2013). Their abundance usually peaks at the oxic/anoxic boundary and they have been shown to be the dominant bacteria in some environments (e.g., Spring *et al.*, 1993; Simmons *et al.*, 2007). They have received much attention in the context of the search for ancient traces of life (e.g., Li *et al.*, 2013). They sometimes contribute significantly to the sediment magnetic signal (Chen *et al.*, 2014). However, their effective impact on geochemical cycles has been rarely assessed (Lin *et al.*, 2014) except in a study by Chen *et al.* (2014) suggesting that MTB-associated Fe may provide a significant iron flux in some euxinic systems.

Lake Pavin is a permanently stratified (meromictic) crater lake with a maximum depth of 92 m. The oxic/anoxic boundary is located within the water column, shifting in depth

between ~50 to ~65 m depending on the efficiency of water mixing (Michard *et al.*, 1994). In contrast with many permanently stratified water bodies which are euxinic below their chemocline, the monimolimnion of Lake Pavin is ferruginous, *i.e.* sulphide-poor (<20 µM; Bura-Nakić *et al.*, 2009) and Fe(II)-rich (up to 1200 µM; Busigny *et al.*, 2016). The P and Fe cycles are tightly coupled in the anoxic zone through precipitation of Fe phosphates, which impacts the concentration of dissolved P in the deep anoxic waters (Cosmidis *et al.*, 2014; Fig. S-1).

Strong chemical gradients in the water column of Lake Pavin (Fig. S-1) parallel a broad diversity of mineral phases associated with microorganisms, including MTB (Miot *et al.*, 2016). Because the oxic-anoxic interface occurs within the water column of Lake Pavin, it is easily accessible compared to many other aqueous environments, where it is located within the sediments. We therefore studied MTB at the oxic-anoxic interface in Lake Pavin and particularly focused on their association with phosphorus.

1. Institut de Minéralogie, de Physique des Matériaux, et de Cosmochimie (IMPMC), Sorbonne Universités, UPMC Université Paris 6, UMR CNRS 7590, Muséum National d'Histoire Naturelle, IRD UMR 206, 4 place Jussieu, 75005 Paris, France
- \* Corresponding author (email: karim.benzerara@upmc.fr)
2. CNRS/CEA/Aix-Marseille Université, UMR7265 Biosciences and Biotechnologies Institute, 13108 Saint Paul lez Durance, France
3. Institut de Physique du Globe de Paris (IPGP), Sorbonne Paris Cité– Université Paris Diderot, UMR CNRS 7154, 1 rue Jussieu, 75238 Paris cedex 05, France
4. Synchrotron SOLEIL, Lucia Beamline, 91192 Gif Sur Yvette, France



## Results

MTB cells were detected by optical microscopy in non-sorted and magnetically-sorted samples collected between 53 and 59 m depth. All MTB-containing samples were collected at a depth where  $O_2$  concentration was lower than the detection limit of the probe (Fig. S-1). Over the sampled depth range, total dissolved Fe, DIP and  $H_2S$  concentrations increased from 0.2 to  $\sim 60 \mu M$ , 0.3 to  $\sim 20 \mu M$  and 0 to  $\sim 2.5 \mu M$ , respectively. MTB populations reached a maximum concentration of  $1.4 \times 10^3$  cells/mL. This can be compared to the total number of bacterial cells ranging between  $2 \times 10^6$  and  $9 \times 10^6$  cells/mL in the oxic-anoxic transition zone of Lake Pavin as estimated by Lehours *et al.* (2005). In the MTB population, small curved rods and large rods were observed, but the majority of MTB cells collected at the oxycline were cocci measuring  $\sim 2 \mu m$  in diameter. Several morphotypes of MTB cocci were observed: the most common contained 1) two chains of cuboctahedral magnetosomes, while some others contained 2) four magnetosome chains or 3) magnetite crystals not aligned as chains

(Fig. 1). Many of these MTB cells contained two other types of electron dense granules: S-rich and P-rich granules. S-granules were not systematically observed, although granules that contained only S are shown by EDXS and measured up to  $\sim 820$  nm in diameter (Fig. S-2). In many MTB cocci, P-rich inclusions filled most of the volume of the cells (Figs. 1, S-2). P-granules contained Ca, K, Mg and P with varying relative abundances. Some MTB cells contained Mg-rich P-granules with relative abundances of Mg, P, K and Ca of  $22.8 \pm 4$ ,  $65.9 \pm 3.2$ ,  $5.1 \pm 3.1$  and  $6 \pm 5.4$  at. % ( $n = 37$ ), respectively. Other MTB cells contained P-granules poorer in Mg and richer in Ca with relative abundances of Mg, P, K and Ca of  $6.7 \pm 2.5$ ,  $56 \pm 3.4$ ,  $1.5 \pm 0.7$  and  $35.3 \pm 1.9$  at. % ( $n = 11$ ), respectively. Similar P-granules have been classically interpreted as polyphosphates (polyP), which are linear polymers of orthophosphate linked by high energy phosphoanhydride bonds (Kornberg, 1995). The  $(K + Mg + Ca)/P$  ratio ( $< 0.8$ ) is suggestive of polyphosphates. Here, this interpretation was confirmed by DAPI staining (Figs. 2, S-3).

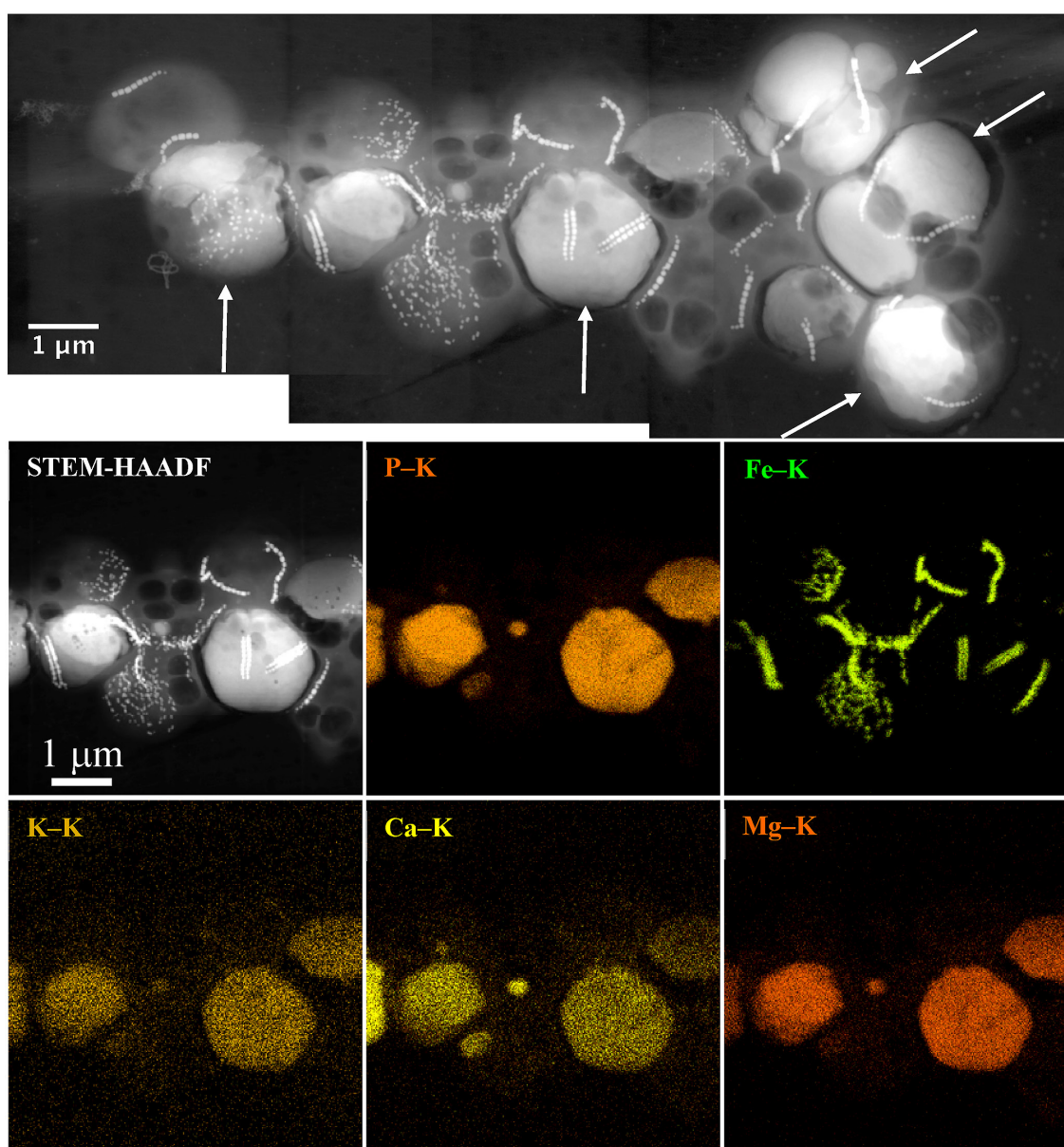


**Figure 1** Scanning transmission electron microscopy analyses of MTB cells at the oxic-anoxic interface in Lake Pavin. **Top:** STEM-HAADF image showing a cluster of MTB cells. Magnetites are the brightest particles. Some cells contain two or four magnetite chains; some (bottom left) contain scattered magnetite. Polyphosphates appear as bright granules filling completely some of the cells (e.g., arrows). **Bottom:** EDXS maps.

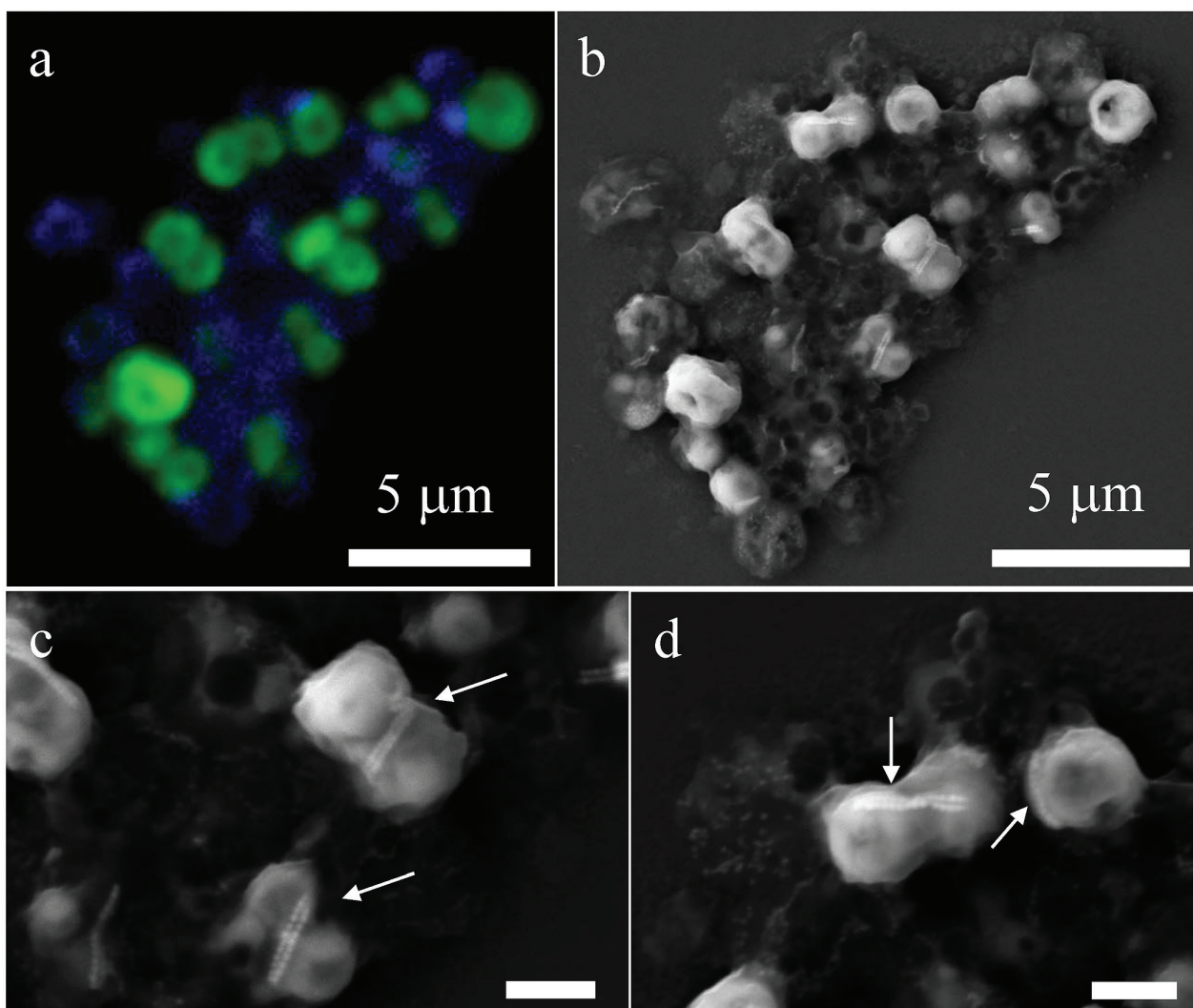


**Figure 2** Correlative CLSM-SEM microscopy. (a) Overlay of fluorescence maps of DAPI-stained nucleic acid (blue) and polyphosphate (green). (b) SEM image in secondary electron mode of the same area. Brighter cells are filled with polyphosphates. (c) and (d) Close ups of areas seen in (b). Cells filled with polyphosphates contain bright magnetite chains (arrows). Scale bar is 1  $\mu\text{m}$  for (c) and (d).

Phylogenetic analyses revealed that the dominant operational taxonomic units (OTU) from magnetically enriched samples were affiliated to Alphaproteobacteria and more specifically, the *Magnetococcaceae* family (Fig. 3). Based on a similarity threshold of 99 % on the whole 16S rDNA gene sequence for defining species, two different species of magnetotactic cocci were detected. One species (8 clones, accession numbers KX270016-KX270023), represented the most abundant MTB at the oxycline of Lake Pavin. The closest relatives were two magnetotactic cocci (GQ468510 and GQ468517) previously detected in the sediments of Lake Miyun (Beijing, China; Lin *et al.*, 2010). A second species found in smaller proportions (accession number KX270015) was closely related to OTU 13, another magnetotactic coccus detected in Lake Miyun (GQ468512).

In order to better assess the significance of the phosphorus fraction carried by these MTB cells, total particulate matter ( $>0.2 \mu\text{m}$ ) was collected at the Lake Pavin oxic-anoxic interface and analysed by synchrotron-based x-ray microfluorescence (Fig. 4). The integrated fluorescence intensity at each pixel of the P map was linearly related to the amount of P. We identified 41 areas with high P contents (Fig. S-4). Some areas consisted of a single pixel, whereas others comprised as many as 40 contiguous pixels. All these areas were systematically re-analysed correlatively at higher spatial resolution by SEM. Eight of these P hotspots corresponded to polyP-loaded

MTB cells (Fig. 4b,c,e,g,i-l; Fig. S-4). Four other less intense P hotspots were also polyP-loaded MTB cells (Fig. 4a,d,f,h). All the other P hotspots were Fe phosphate precipitates and no other microorganism was detected among these P hotspots (Fig. S-5). Altogether, the 12 polyP-loaded MTB cells identified by SEM harboured 0.6 % of the total P in the mapped area, which comprises a total of 21,336 pixels. Moreover, the P content measured on single MTB-containing pixels was between 6- and 23-fold higher than the median *per pixel* P content (Fig. S-6), providing a rough assessment of the P concentration factor in MTB compared to other cells.

## Discussion

Here, we show that some MTB accumulate polyP to a very high level, up to  $\sim 23$ -fold higher than most microbial cells found at the oxic-anoxic interface in the water column of Lake Pavin. High accumulation of polyP was previously documented for several, non-MTB, bacterial species belonging to Proteobacteria and Actinobacteria (*e.g.*, Nakamura *et al.*, 1995; He and McMahon, 2011). Such bacteria have been considered as critical actors for the removal of excess phosphorus from wastewater (Tarayre *et al.*, 2016) or the formation of marine P-rich sediments called phosphorites (Crosby and Bailey, 2012).

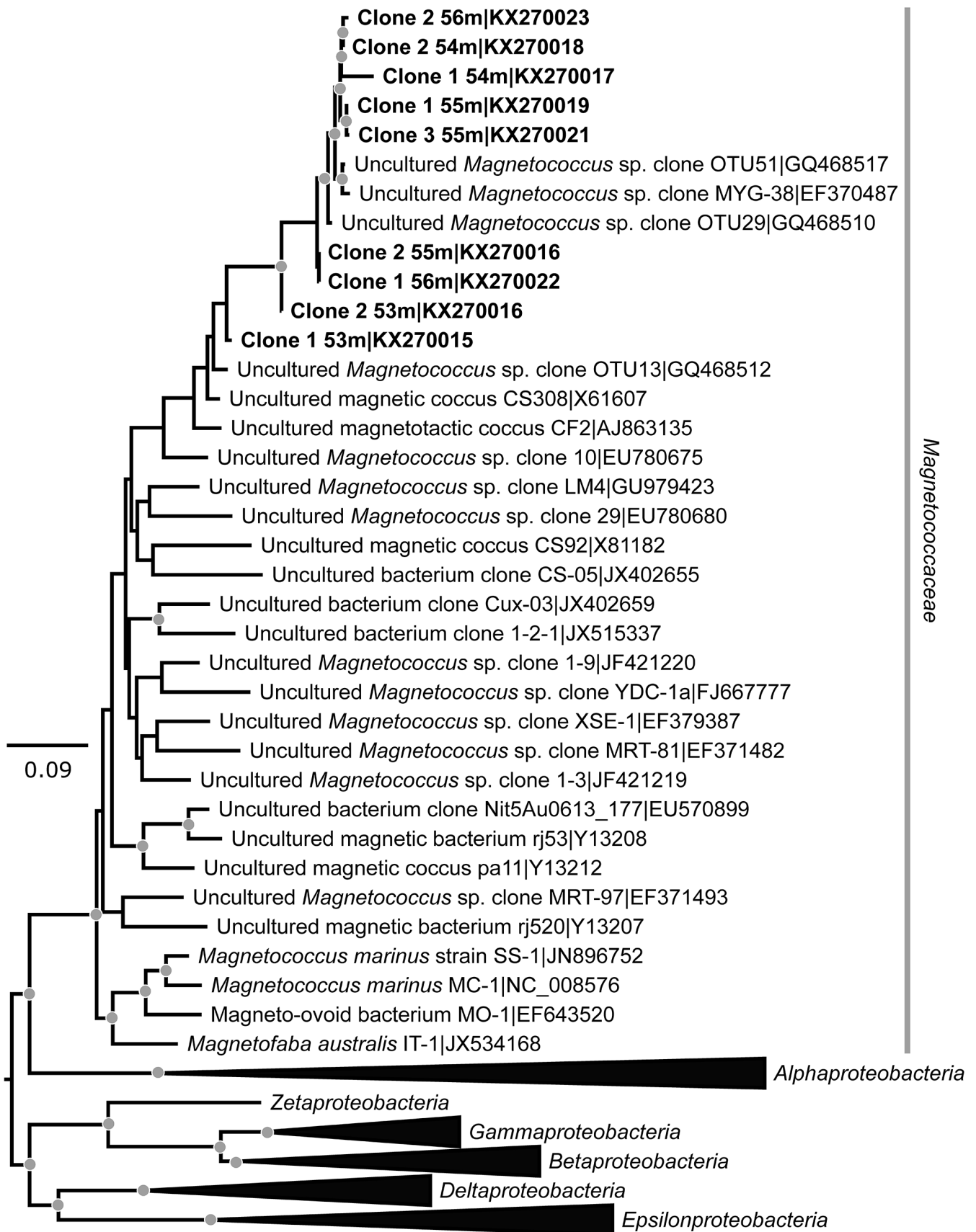


**Figure 3** Maximum likelihood phylogenetic tree built based on 16S rDNA gene sequences of MTB clones from Lake Pavin (bold). It includes the closest related *Magnetococcaceae* found elsewhere. GenBank accession numbers are associated with clones/strains names. Nodes supported by a bootstrap value above 70 % are highlighted by a grey circle. Branch length is proportional to the number of base substitutions per site (see scale bar).

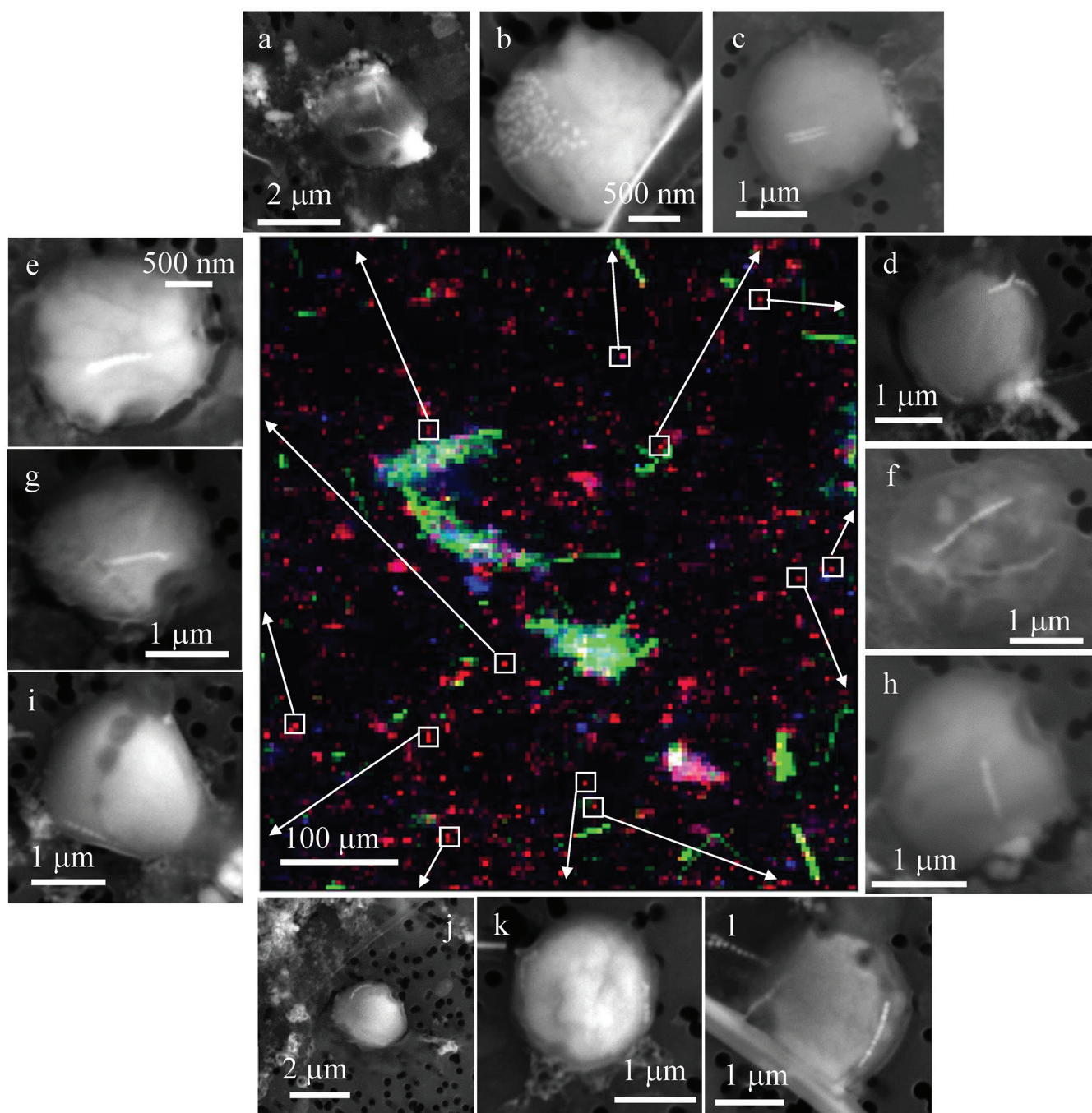


**Figure 4** Correlative  $\mu$ -XRF and SEM microscopy. **Centre:** XRF maps of P (red), Si (green) and S (blue). The brightest P spots were subsequently imaged by SEM. Many hotspots correspond to polyP-loaded MTB cells as shown in (a) to (l). Other hotspots were almost exclusively Fe phosphate precipitates (Fig. S-5).

Some magnetotactic cocci from Lake Baldwin, California and Itaipu lagoon, Brazil resembling the MTB cells observed in Lake Pavin were also shown to form intracellular polyP inclusions, sometimes occupying a large part of their cell volume (Cox *et al.*, 2005; Keim *et al.*, 2005). This process is even more pronounced in Lake Pavin with some *Magnetococcaceae* cells fully filled with polyP. Here, the ability of these cells to swim along the magnetic field lines during magnetic enrichment procedures suggests that they stay viable.

Several functions have been suggested for polyP inclusions such as a source of ATP, or a response to oxidative stress (Seviour *et al.*, 2003). MTB cells containing large amounts of polyP in Lake Pavin were detected at depths where low extracellular P concentrations ( $\sim 0.7 \mu\text{M}$  at 54 m) were measured. Several environmental conditions have been shown to

stimulate polyP accumulation/hydrolysis (*e.g.*, Brock and Schulz-Vogt, 2011). Firstly, in wastewater treatments, addition of fatty acids or acetate under anoxic conditions triggers phosphate release by some polyP-concentrating bacteria (Comeau *et al.*, 1986), while these bacteria accumulate polyP under oxic conditions (*e.g.*, Karl *et al.*, 2014). Oxic-anoxic cycles induce high polyP accumulation in these bacteria. Lake Pavin *Magnetococcaceae* may massively accumulate polyP by experiencing similar oxic/anoxic fluctuations, either by travelling vertically over short distances from the oxic to anoxic zone (and *vice versa*), or by being affected by seasonal depth shifts of the oxic/anoxic boundary. Accumulation and hydrolysis of polyP may affect cell buoyancy as shown for other bacteria (Romans *et al.*, 1994) and favour downward movements after accumulation. Secondly, and alternatively, addition of sulphide under anoxic conditions triggers phosphate release by the sulphoxidising

bacteria *Beggiatoa* and *Thiomargarita* (Brock and Schulz-Vogt, 2011), while these bacteria accumulate and keep high polyP contents under oxic conditions and anoxic sulphide-poor conditions. Interestingly, intracellular S-globules in some of Lake Pavin MTB cells suggest that these bacteria are sulphide and/or thiosulphate oxidisers, similar to the closely genetically related cultured *Magnetococcus marinus* strain MC-1 (Bazylnski *et al.*, 2013). Whether Lake Pavin MTB are affected by sulphides similarly to *Beggiatoa* will have to be determined. If this is the case, sulphide concentrations are relatively low (<0.2  $\mu\text{M}$  below 58 m) at the depth where Lake Pavin MTB were observed and could be a parameter explaining the high accumulation of polyP in MTB below the oxic/anoxic boundary in Lake Pavin. Analysing the polyP content of MTB cells at different depths throughout these chemical gradients would help in answering this question.

Fe phases were suggested to control the P geochemical cycle in Lake Pavin (Busigny *et al.*, 2016) via high affinity sorption at their surface. Alternatively, involvement of microorganisms in the extracellular precipitation of Fe phosphates has been evidenced (Cosmidis *et al.*, 2014; Miot *et al.*, 2016). Here, MTB also couple the geochemical cycles of P and Fe through accumulation of two separate Fe and P intracellular reservoirs (polyP and magnetites).

The geochemical impact of polyP-accumulating bacteria has been particularly stressed in the context of wastewater treatment and the formation of phosphorites. In the first case, bacterial genera such as *Pseudomonas* and *Acinetobacter* play a predominant role in P accumulation in P-rich solutions (Nathan *et al.*, 1993). In the case of marine phosphorite formation, sulphoxidising bacteria have become major bacterial models involved in the accumulation of low concentrations of P from the water column, before release in porewater under anoxic conditions, resulting in the precipitation of apatite-like phases in the sediments (Goldhammer *et al.*, 2010). Microfossils resembling modern sulphoxidising bacteria were evidenced in the geological record, suggesting that they may have played a role in the formation of ancient phosphorites as well (Bailey *et al.*, 2013). Diatoms have been also suspected to be major players in the accumulation of P as polyP, before release and precipitation of P phases in the sediments (Diaz *et al.*, 2008). Here, we show that *Magnetococcaceae* appear as new models of polyP-accumulating bacteria in freshwater ferruginous environments. While the reservoir they represent seems modest in size (<1 % of the total P), it may, similarly to sulphoxidising bacteria in some marine sediments, be dynamic because of active microbially mediated transformations of polyP and may therefore significantly contribute to the P cycle in this environment. This will be important to assess further in future studies. The relative simplicity by which MTB can be extracted from a suspension by magnetic sorting makes them an interesting tool for concentrating and removing P from a solution. Moreover, similar to sulphide oxidising bacteria, traces of MTB are tractable in the geological record. Identifying the specific crystallographic, geochemical and/or magnetic properties (*e.g.*, Amor *et al.*, 2016) of their intracellular magnetites provides a perspective to track their potential contribution to the formation of ancient lacustrine phosphorites.

## Acknowledgements

KB has been supported by funding from the European Research Council under the European Community's Seventh Framework Programme (FP7/2007-2013 Grant Agreement no.307110 – ERC CALCYAN). The TEM and SEM facilities at IMPMC were purchased owing to a support by Region Ile-de-France grant SESAME 2000E1435 and 2006N°I-07-593/R. CM and

CL were supported by the French National Research Agency (ANR Tremplin-ERC BIOMAGNET and ANR MEFISTO). ED was supported by the French National Center for Scientific Research (CNRS-INSU program EC2CO). JM was supported by the ANR SRB project, grant ANR-14-CE33-0003-01 of the French Agence Nationale de la Recherche.

Editor: Liane G. Benning

## Additional Information

**Supplementary Information** accompanies this letter at [www.geochemicalperspectivesletters.org/article1743](http://www.geochemicalperspectivesletters.org/article1743)

**Reprints and permission information** are available online at <http://www.geochemicalperspectivesletters.org/copyright-and-permissions>

**Cite this letter as:** Rivas-Lamelo, S., Benzerara, K., Lefèvre, C.T., Monteil, C.L., Jézéquel, D., Menguy, N., Viollier, E., Guyot, F., Féraud, C., Poinot, M., Skouri-Panet, F., Trcera, N., Miot, J., Duprat, E. (2017) Magnetotactic bacteria as a new model for P sequestration in the ferruginous Lake Pavin. *Geochem. Persp. Lett.* 5, 35–41.

## References

- AMOR, M., BUSIGNY, V., LOUVAT, P., GELABERT, A., CARTIGNY, P., DURAND-DUBIEF, M., ONA-NGUEMA, G., ALPHANDERY, E., CHEBBI, I., GUYOT, F. (2016) Mass-dependent and -independent signature of Fe isotopes in magnetotactic bacteria. *Science* 352, 705–708.
- BAILEY, J.V., CORSETTI, F. A., GREENE, S.E., CROSBY, C.H., LIU, P., ORPHAN, V.J. (2013) Filamentous sulfur bacteria preserved in modern and ancient phosphatic sediments: implications for the role of oxygen and bacteria in phosphogenesis. *Geobiology* 11, 397–405.
- BAZYLINSKI, D.A., WILLIAMS, T.J., LEFÈVRE, C.T., BERG, R.J., ZHANG, C.L., BOWSER, S.S., DEAN, A.J., BEVERIDGE, T.J. (2013) *Magnetococcus marinus* gen. nov., sp. nov., a marine, magnetotactic bacterium that represents a novel lineage (Magnetococcales ord. nov.) at the base of the Alphaproteobacteria. *International Journal of Systematic and Evolutionary Microbiology* 63, 801–808.
- BLAKEMORE, R. (1975) Magnetotactic bacteria. *Science* 190, 377–379.
- BROCK, J., SCHULZ-VOGT, H.N. (2011) Sulfide induces phosphate release from polyphosphate in cultures of a marine *Beggiatoa* strain. *ISME Journal* 5, 497–506.
- BURA-NAKIĆ, E., VIOLLIER, E., JÉZÉQUEL, D., THIAM, A., CIGLENE KI, I. (2009) Reduced sulfur species in anoxic water column of meromictic Pavin crater lake (Massif Central, France). *Chemical Geology* 266, 311–317.
- BUSIGNY, V., MICHARD, G., JÉZÉQUEL, D., COSMIDIS, J., VIOLLIER, E., BENZERARA, K., PLANAVSKY, N.J., ALBÉRIC, P., LEBEAU, O., SARAZIN, G. (2016) The iron wheel in Lac Pavin: interaction with phosphorus cycle. In: Sime-Ngando, T., Boivin, P., Chapron, E., Jezequel, D., Meybeck, M. (Eds.) *Lake Pavin*. Springer International Publishing, Switzerland, 205–220.
- CHEN, A.P., BEROUNSKY, V.M., CHAN, M.K., BLACKFORD, M.G., CADY, C., MOSKOWITZ, B.M., KRAAL, P., LIMA, E.A., KOPP, R.E., LUMPKIN, G.R., WEISS, B.P., HESSE, P., VELLA, N.G.F. (2014) Magnetic properties of uncultivated magnetotactic bacteria and their contribution to a stratified estuary iron cycle. *Nature Communications* 5, 4797.
- COMEAU, Y., HALL, K.J., HANCOCK, R.E.W., OLDHAM, W.K. (1986) Biochemical-model for enhanced biological phosphorus removal. *Water Research* 20, 1511–1521.
- COSMIDIS, J., BENZERARA, K., MORIN, G., BUSIGNY, V., LEBEAU, O., JÉZÉQUEL, D., NOËL, V., DUBLET, G., OTHMANE, G. (2014) Biomineralization of iron-phosphates in the water column of Lake Pavin (Massif Central, France). *Geochimica et Cosmochimica Acta* 126, 78–96.
- COX, B.L., POPA, R., BAZYLINSKI, D.A., LANOIL, D., DOUGLAS, S., BELZ, A., ENGLER, D.L., NEALSON, K.H. (2002) Organization and elemental analysis of P-, S-, and Fe-rich inclusions in a population of freshwater magnetococci. *Geomicrobiology Journal* 19, 387–406.



- CROSBY, C.H., BAILEY, J.V. (2012) The role of microbes in the formation of modern and ancient phosphatic mineral deposits. *Frontiers in Microbiology* 3, 241.
- DIAZ, J., INGALL, E., BENITEZ-NELSON, C., PATERSON, D., DE JONGE, M.D., MCNULTY, I., BRANDES, J.A. (2008). Marine polyphosphate: a key player in geologic phosphorus sequestration. *Science* 320, 652–655.
- GOLDHAMMER, T., BREUCHERT, V., FERDELMAN, T.G., ZABEL, M. (2010) Microbial sequestration of phosphorus in anoxic upwelling sediments. *Nature Geoscience* 3, 557–561.
- HE, S., MCMAHON, K.D. (2011) Microbiology of “Candidatus Accumulibacter” in activated sludge. *Microbial Biotechnology* 4, 603–619.
- KARL, D.M. (2014) Microbially Mediated Transformations of Phosphorus in the Sea: New Views of an Old Cycle. *Annual Review of Marine Science* 6, 279–337.
- KEIM, C.N., SOLORZANO, G., FARINA, M., LINS, U. (2005) Intracellular inclusions of uncultured magnetotactic bacteria. *International Microbiology* 8, 111–117.
- KORNBERG, A. (1995). Inorganic polyphosphate—toward making a forgotten polymer unforgettable. *Journal of Bacteriology* 177, 491–496
- LEFÈVRE, C.T., BAZYLINSKI, D.A. (2013) Ecology, Diversity, and Evolution of Magnetotactic Bacteria. *Microbiology and Molecular Biology Reviews* 77, 497–526.
- LEHOURS, A.C., BARDOT, C., THENOT, A., DEBROAS, D., FONTY, G. (2005) Anaerobic microbial communities in Lake Pavin, a unique meromictic lake in France. *Applied and Environmental Microbiology* 71, 7389–7400.
- LI, J., BENZERARA, K., BERNARD, S., BEYSSAC, O. (2013) The link between biomineralization and fossilization of bacteria: Insights from field and experimental studies. *Chemical Geology* 359, 49–69.
- LIN, W., PAN, Y. (2010) Temporal variation of magnetotactic bacterial communities in two freshwater sediment microcosms. *FEMS Microbiology Letters* 302, 85–92.
- LIN, W., BAZYLINSKI, D.A., XIAO, T., WU, L.F., PAN, Y.X. (2014) Life with compass: diversity and biogeography of magnetotactic bacteria. *Environmental Microbiology* 16, 2646–2658.
- MICHARD, G., VIOLLIER, E., JEZEQUEL, D., SARAZIN, G. (1994) Geochemical study of a crater lake - Pavin lake, France - identification, location and quantification of the chemical-reactions in the lake. *Chemical Geology* 115, 103–115.
- MIOT, J., JEZEQUEL, D., BENZERARA, K., CORDIER, L., RIVAS-LAMELO, S., SKOURI-PANET, F., FERARD, C., POINSOT M., DUPRAT, E. (2016) Mineralogical diversity in Lake Pavin: connections with water column chemistry and biomineralization processes. *Minerals* 6, 24.
- NAKAMURA, K., HIRAISHI, A., YOSHIMI, Y., KAWAHARASAKI, M., MASUDA, K., KAMAGATA, Y. (1995) *Microlunatus phosphovorius* gen. nov., sp. nov., a new gram-positive polyphosphate-accumulating bacterium isolated from activated sludge. *International Journal of Systematic and Evolutionary Microbiology* 45, 17–22.
- NATHAN, Y., BREMNER, J.M., LOWENTHAL, R.E., MONTEIRO, P. (1993) Role of bacteria in phosphorite genesis. *Geomicrobiology Journal* 11, 69–76.
- ROMANS, K.M., CARPENTER, E.J., BERGMAN, B. (1994) Buoyancy regulation in the colonial diazotrophic cyanobacterium *Trichodesmium tenue*: ultrastructure and storage of carbohydrate, polyphosphate, and nitrogen. *Journal of Phycology* 30, 935–942.
- SEVIOUR, R.J., MINO, T., ONUKI, M. (2003) The microbiology of biological phosphorus removal in activated sludge systems. *FEMS Microbiology Review* 27, 99–127.
- SIMMONS, S.L., BAZYLINSKI, D.A., EDWARDS, K.J. (2007) Population dynamics of marine magnetotactic bacteria in a meromictic salt pond described with qPCR. *Environmental Microbiology* 9, 2162–2174.
- SPRING, S., AMANN, R., LUDWIG, W., SCHLEIFER, K.H., VAN GEMERDEN, H., PETERSEN, N. (1993) Dominating role of an unusual magnetotactic bacterium in the microaerobic zone of a freshwater sediment. *Applied and Environmental Microbiology* 59, 2397–2403.
- TARAYRE, C., NGUYEN H.T., BROGNAUX, A., DELEPIERRE, A., DE CLERCQ, L., CHARLIER, R., MICHELS, E., MEERS, E., DELVIGNE, F. (2016) Characterization of Phosphate Accumulating Organisms and Techniques for Polyphosphate Detection: A Review. *Sensors* 16, 797.



## Magnetotactic bacteria as a new model for P sequestration in the ferruginous Lake Pavin

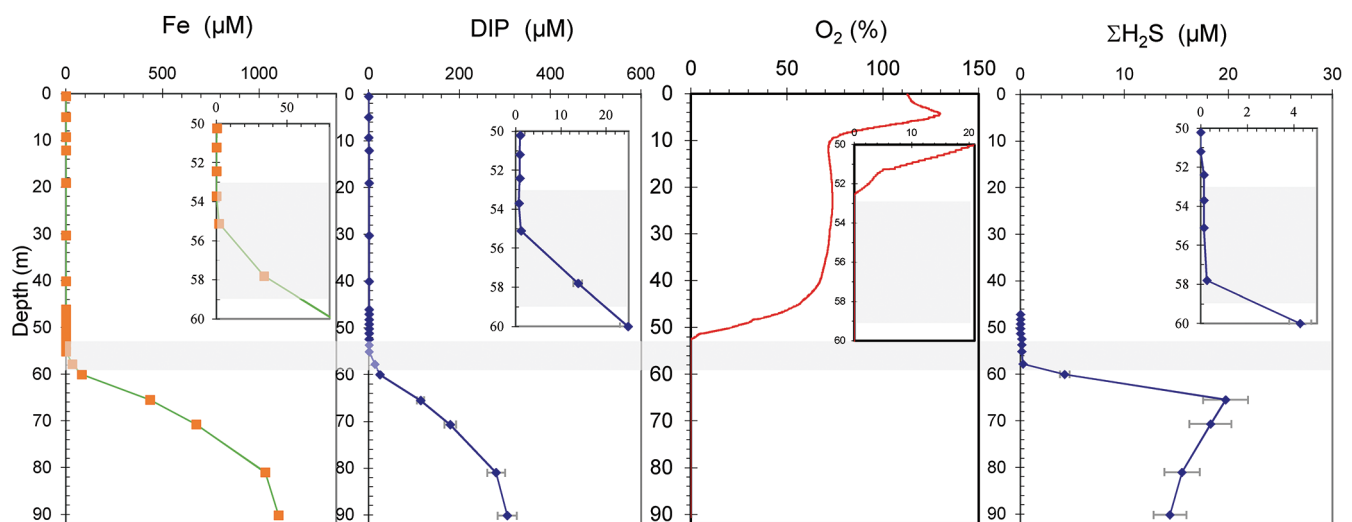
S. Rivas-Lamelo<sup>1</sup>, K. Benzerara<sup>1\*</sup>, C.T. Lefèvre<sup>2</sup>, C.L. Monteil<sup>2</sup>,  
D. Jézéquel<sup>3</sup>, N. Menguy<sup>1</sup>, E. Viollier<sup>3</sup>, F. Guyot<sup>1</sup>, C. Férard<sup>1</sup>, M. Poinso<sup>1</sup>,  
F. Skouri-Panet<sup>1</sup>, N. Trcera<sup>4</sup>, J. Miot<sup>1</sup>, E. Duprat<sup>1</sup>

### Supplementary Information

The Supplementary Information includes:

- Supplementary Data
- Material and Methods
- Figures S-1 to S-6
- Supplementary Information References

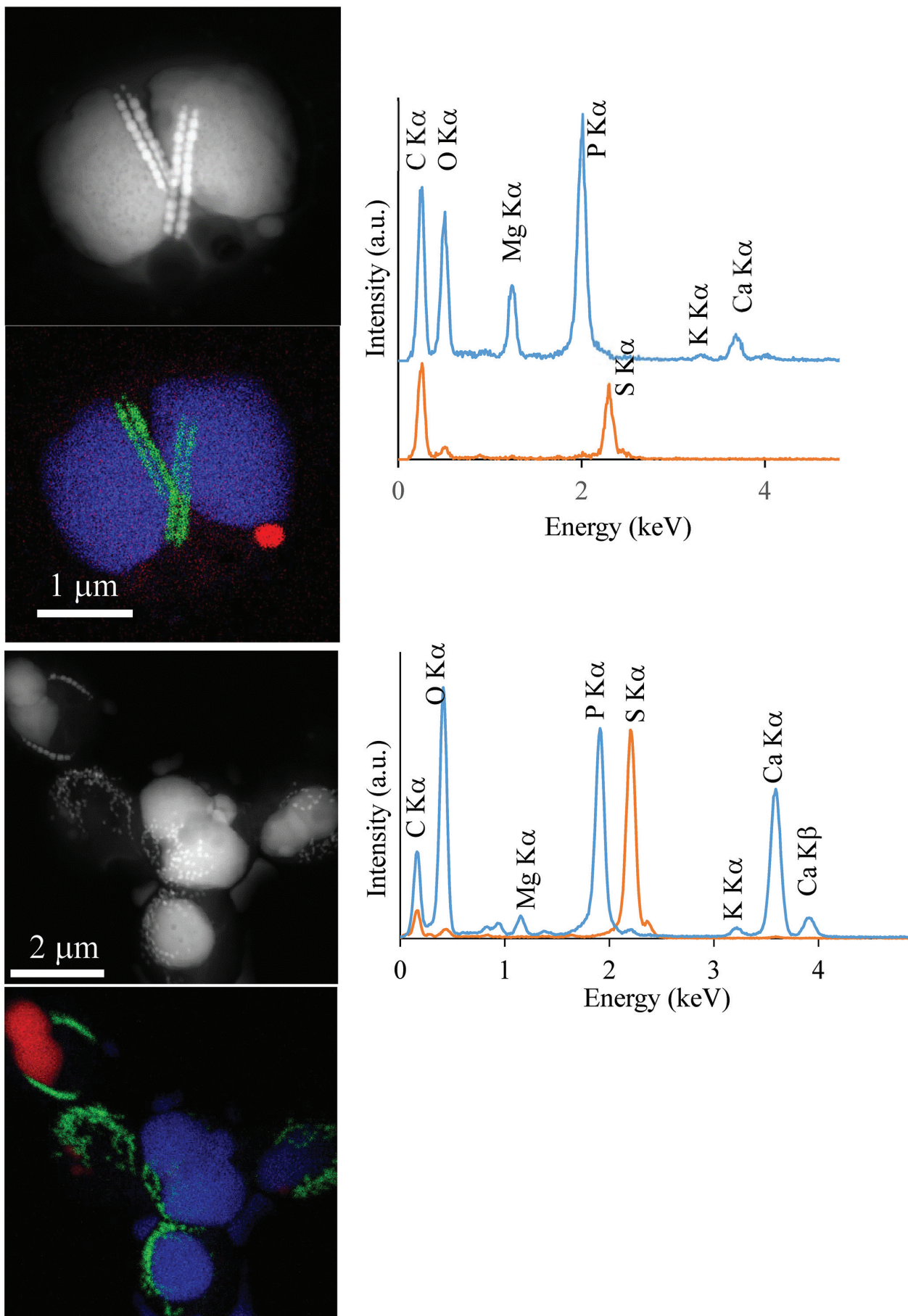
### Supplementary Data



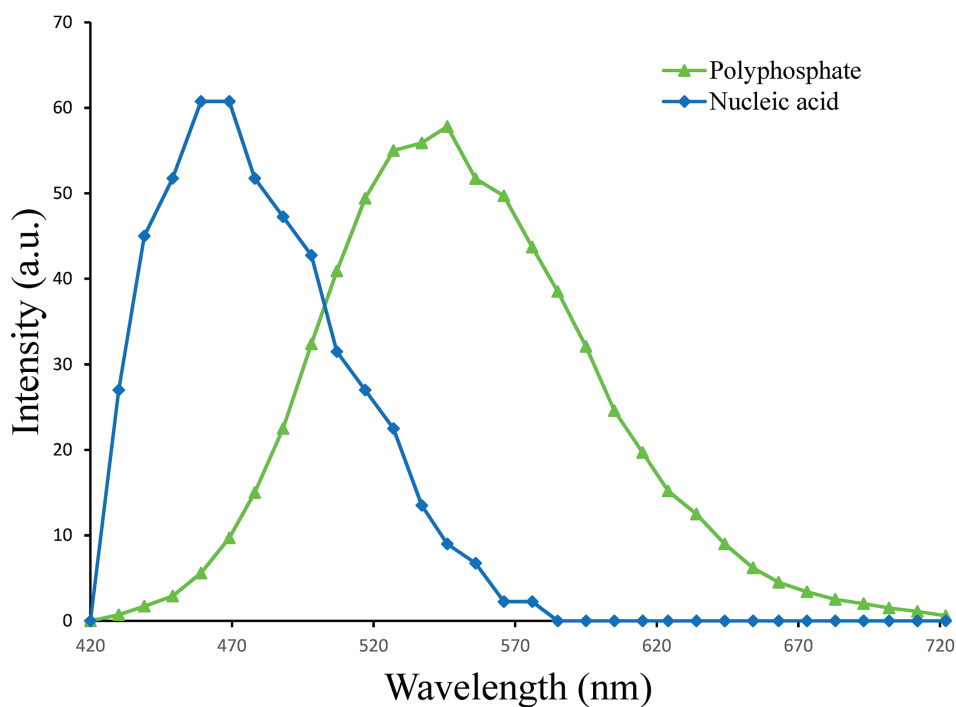
**Figure S-1** Geochemical depth profiles in the water column of Lake Pavin. The depth profile of O<sub>2</sub> was measured *in situ*, while depth profiles of dissolved H<sub>2</sub>S (ΣH<sub>2</sub>S), dissolved PO<sub>4</sub> (DIP) and dissolved Fe<sup>2+</sup> were measured on water samples collected using a Niskin bottle. The grey rectangle outlines the depth range in which MTB cells were collected.

1. Institut de Minéralogie, de Physique des Matériaux, et de Cosmochimie (IMPMC), Sorbonne Universités, UPMC Université Paris 6, UMR CNRS 7590, Muséum National d'Histoire Naturelle, IRD UMR 206, 4 place Jussieu, 75005 Paris, France
- \* Corresponding author (email: karim.benzerara@upmc.fr)
2. CNRS/CEA/Aix-Marseille Université, UMR7265 Biosciences and Biotechnologies Institute, 13108 Saint Paul lez Durance, France
3. Institut de Physique du Globe de Paris (IPGP), Sorbonne Paris Cité– Université Paris Diderot, UMR CNRS 7154, 1 rue Jussieu, 75238 Paris cedex 05, France
4. Synchrotron SOLEIL, Lucia Beamline, 91192 Gif Sur Yvette, France

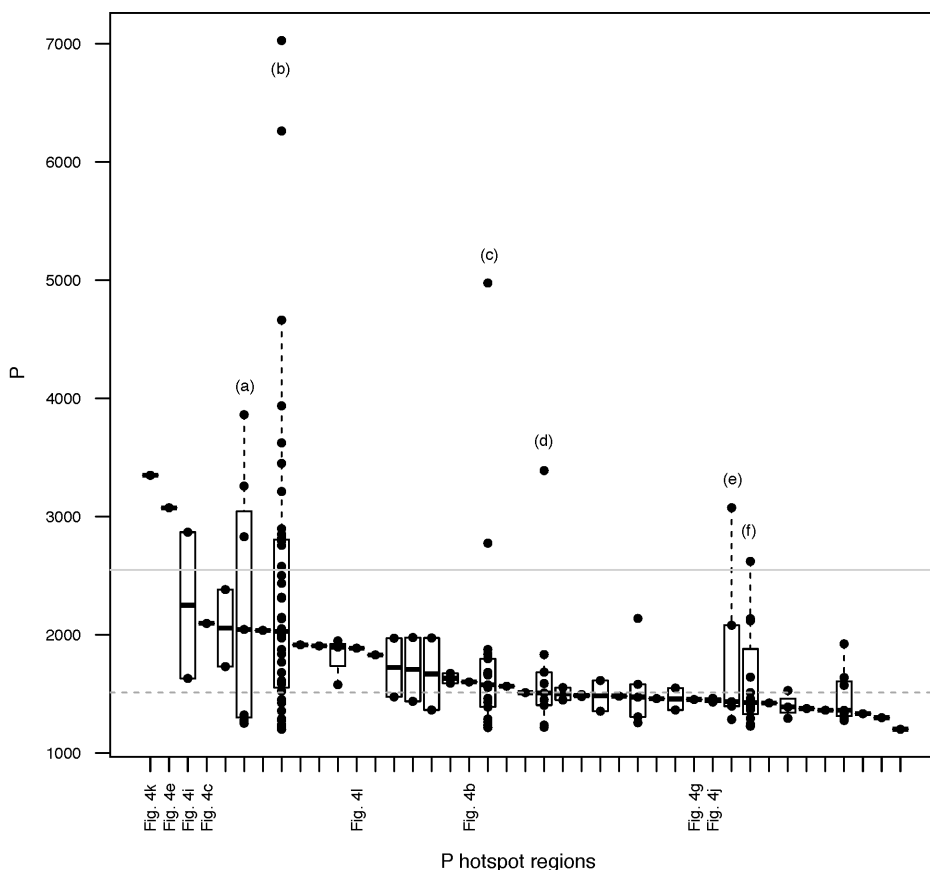




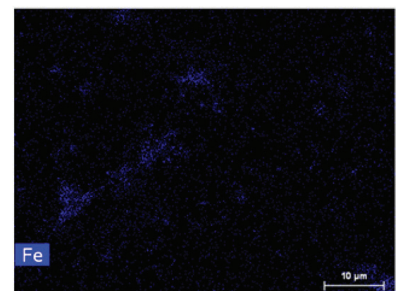
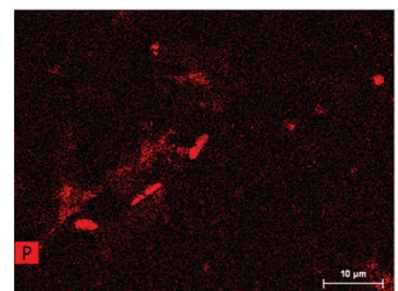
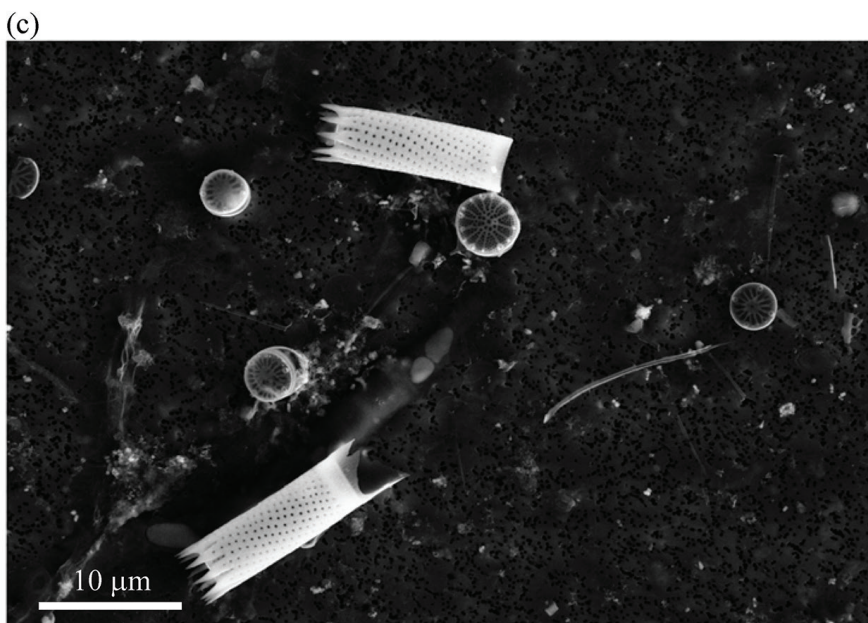
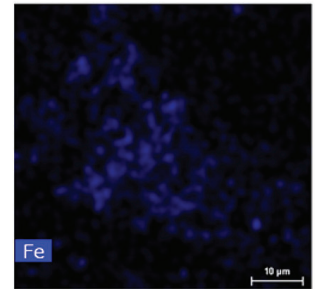
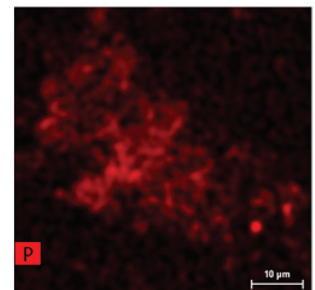
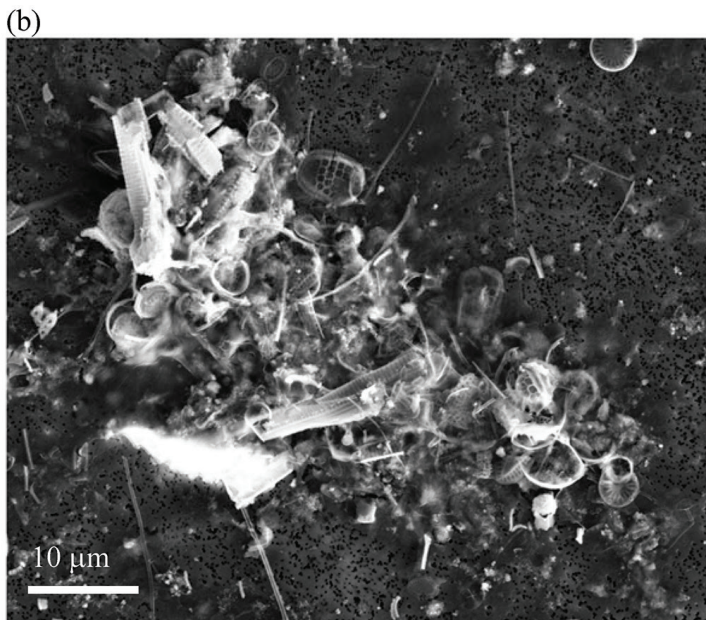
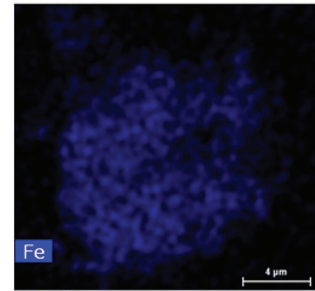
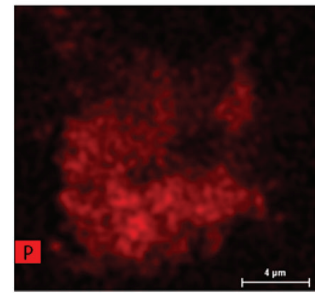
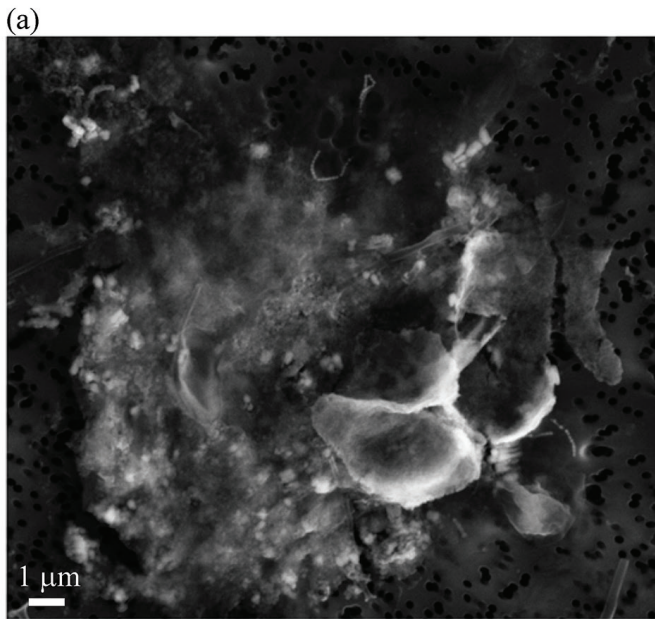
**Figure S-2** STEM and EDXS analyses of polyphosphate and S-granules in MTB cells. **Left:** STEM image in HAADF mode and overlay of Fe (green), P (blue) and S (red) in two different areas. **Right:** EDXS spectra of S-granules (orange) and polyphosphate inclusions (blue).



**Figure S-3** Fluorescence spectra of DAPI-stained nucleic acid (blue) and DAPI-stained polyphosphate (green). Fluorescence maps of the two components as shown in Figure 2a are obtained by measuring fluorescence spectra on each pixel of the image and fitting the resulting spectra as linear combinations of these two reference spectra.



**Figure S-4** Per pixel P distribution of the 41 hotspots, identified from the fitted  $\mu$ -XRF intensity map of P. Hotspots (x-axis) were sorted in descending order according to their median, which is indicated by a bold horizontal line inside each box. X-axis labels (Fig 4x, with x = a, b ...) refer to polyP-loaded MTB cells shown in Figure 4. For a given distribution, the box boundaries indicate the first and third quartiles. The vertical dashed lines that extend from the box encompass the largest/smallest intensities that fall within a distance of 1.5 times the box size from the nearest box hinge. The horizontal gray dashed line at an intensity of 1500 represents the P intensity median of all the hotspots. The hotspots with a high per pixel P content (individual points above the gray horizontal solid line) not related to polyP-loaded MTB cells are described by letters (from a to f); see SEM and EDXS maps of these areas in Figure S-5.



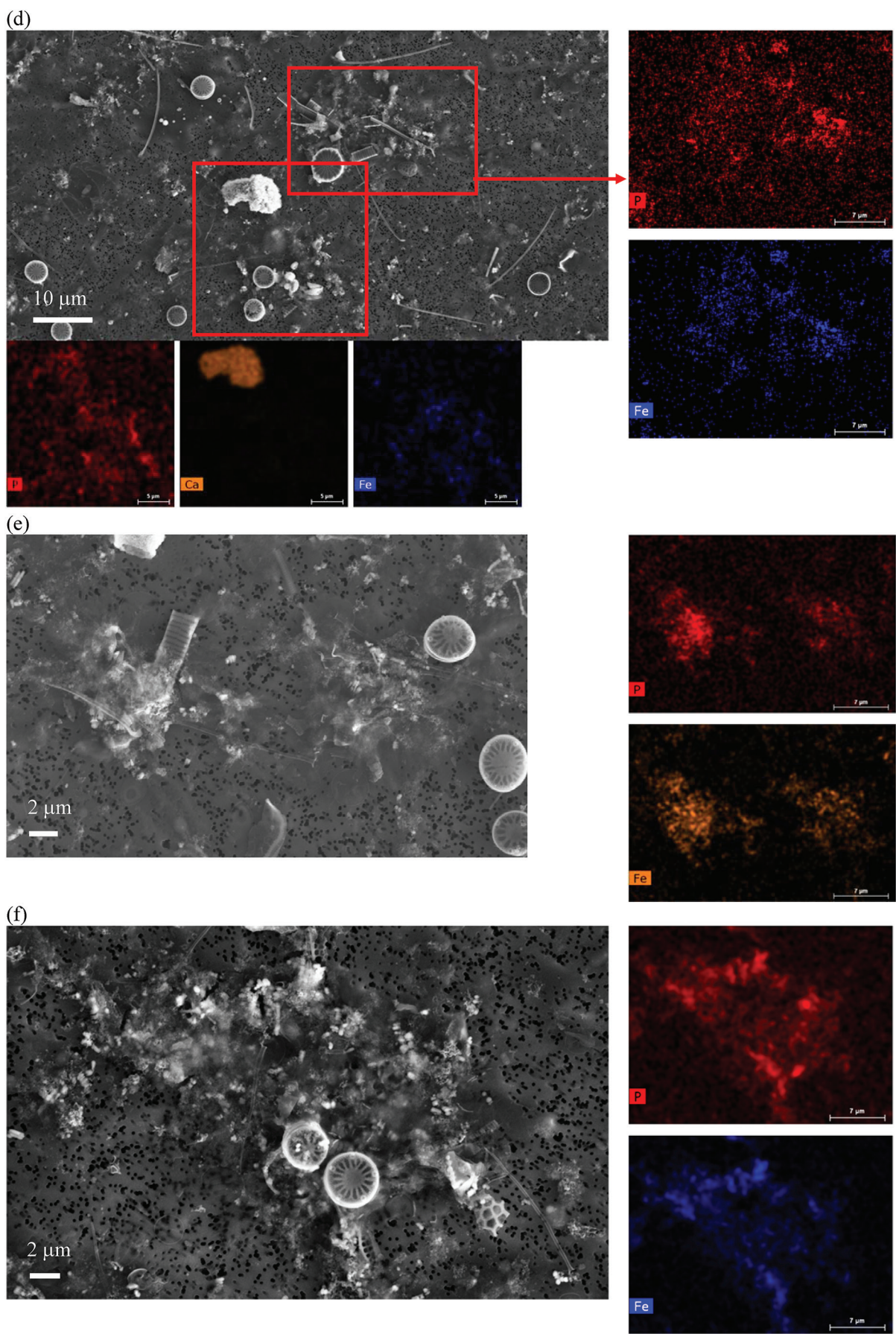


**Figure S-5** SEM and EDXS analyses of P hotspots not related to polyP-loaded MTB cells but containing Fe phosphate phases. These areas are indicated by letters from (a) to (f) in Figure S-4.

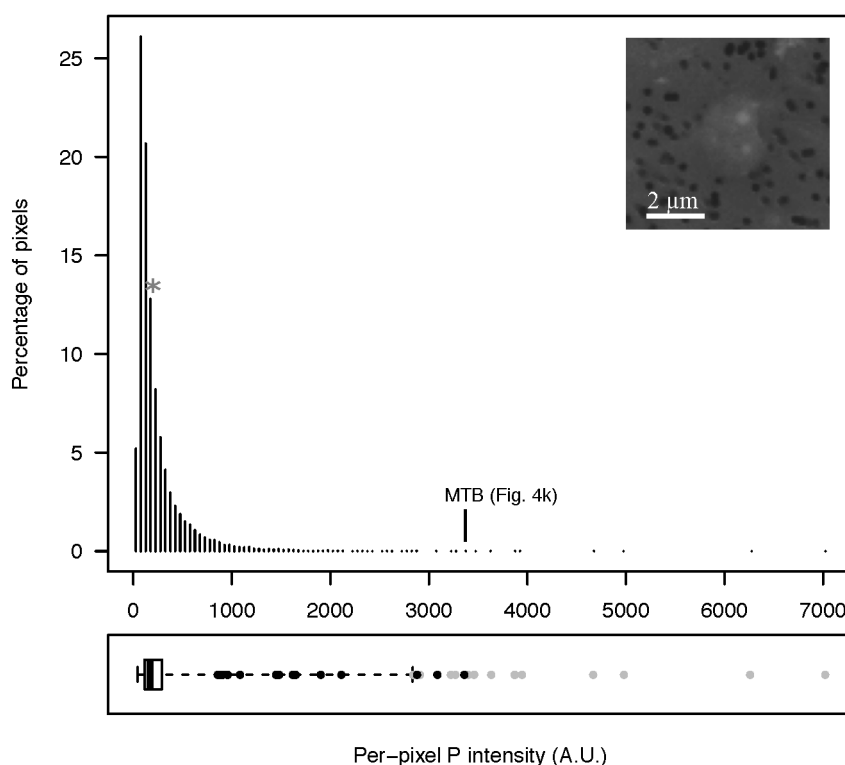


**Figure S-6** Distribution of the *per pixel* P intensity on the  $\mu$ -XRF map shown in Figure 4. Most of the P-containing pixels have a *per pixel* intensity below 144.3 (median value, indicated by a bold vertical line in the bottom box). The MTB-containing pixel with the highest P content (Fig. 4k) is labelled. Below the histogram, the box boundaries indicate the first and third quartiles (*per pixel* intensities of 88.7 and 265.9, respectively). The horizontal dashed line extending to the right encompasses 99.9 % of the P-containing pixels (up to 2826.9). Outliers are represented by individual points. P intensities of the MTB-containing pixels identified by SEM (Fig. 4) are represented by single black dots. On the right, SEM picture of non-MTB microbial cell contained in a pixel with a P intensity of 181.8 (indicated by a grey star above the corresponding histogram bin), *i.e.* slightly above the median.

## Material and Methods

### Aqueous geochemistry and sample collection

Samples were collected in the water column from a platform located at the centre of Lake Pavin (Massif Central, France; 45°29'41" N, 002°53'12" E) with a Niskin bottle in May, June and September 2015. Dissolved oxygen was measured *in situ* using an O<sub>2</sub>-pH-redox probe (YSI 6600). Detection limit for O<sub>2</sub> was 0.1 %. For the analysis of dissolved compounds, water samples were filtered on board using syringes and filters with a Luer connection (Whatman, 0.2  $\mu$ m) and distributed in Falcon® PP tubes (acidified with Suprapur HNO<sub>3</sub> for ICP-AES analysis). The concentration of Fe (total Fe) was measured by ICP-AES (Thermo Scientific iCAP 6200). Sulphides were stabilised by precipitation with zinc (+ 100  $\mu$ L Zn acetate 0.01 M for 10 mL sample). Sulphide species (total H<sub>2</sub>S) determined by this method comprise free H<sub>2</sub>S and HS<sup>-</sup> as well as metal-bound sulphide nanoparticles. The concentrations of DIP (Dissolved Inorganic Phosphorus) (Autoanalyser AxFlow Quattro), and H<sub>2</sub>S (Spectroquant Merck, methylene blue method) were measured by colourimetry.

### Magnetic sorting of MTB cells and sample preparation for STEM analyses

Magnetic enrichment of samples was performed immediately after water collection in a glass bottle. This consisted of placing the south pole of a magnetic stirring bar against the glass bottle. After 3 hr, a white pellet of highly enriched in MTB

cells could be observed close to the magnet. MTB cells were harvested using a pipette, observed and quantified using the hanging drop technique in the laboratory (Schüler, 2002).

### Scanning transmission electron microscopy analyses

STEM analyses of magnetically sorted MTB cells were performed in the high angle annular dark field (HAADF) mode using a JEOL 2100F operating at 200 kV and equipped with a field emission gun and a JEOL EDXS detector. Semi-quantitative analyses of EDXS spectra were processed using the JEOL Analysis Station software following the Li *et al.* (2016) procedure.

### Polyphosphate imaging by DAPI staining

4,6-Diamidino-2-phenylindole dihydrochloride (DAPI) has been commonly used to stain nucleic acids and polyphosphates (Tijssen *et al.*, 1982). Nucleic acids stained by DAPI fluoresce in the blue with a maximum emission at 465 nm. Polyphosphates stained by DAPI fluoresce in the green/yellow with an emission peak centred at ~545 nm (Fig. S-3). 80  $\mu$ L of a DAPI solution at 1 mg/mL was added to 90  $\mu$ L of a magnetically enriched MTB suspension. Incubation was performed for 5 min in the dark before rinsing with milliQ water. A 10  $\mu$ L drop of the suspension was deposited on a glass lamella for confocal laser scanning microscopy (CLSM) analyses. Samples were observed by CLSM using a Zeiss LSM 710. Excitation was performed at 405 nm and emission

spectra were measured for each pixel of the images using a 34 channel Quasar T-PMT detector. Correlation with SEM was performed using the Korrmik Life Sciences sample holder and the correlative Shuttle and Find software implemented in ZEN 2012. Similarly, a study by Eder *et al.* (2014) used a correlative approach of Raman spectromicroscopy and SEM showing an alternative approach to investigate the speciation of P within magnetotactic bacteria.

### Cell count profile

Three 1 L bottles of water were collected every metre above and below the oxycline in order to determine the depth distribution of magnetotactic bacteria (*i.e.* maximum at 56 m on April 7<sup>th</sup> 2016). From each sample, three drops of 40 µL were observed using the hanging drop technique (Schüler, 2002). Magnetotactic cells, accumulating at the edge of the drops due to the magnetic field generated on one side of the drop, were counted under a ZEISS Primo Star light microscope. The number of cells counted in each drop was multiplied by 25 in order to obtain the concentration of cells *per* millilitre.

### Affiliation of dominant MTB populations to a taxonomy rank

MTB cells were concentrated using the magnetic “capillary racetrack” technique (Wolfe *et al.*, 1987). Their 16S rRNA gene was amplified by PCR using the universal pair of primers 27f and 1492r and the Phusion High Fidelity polymerase (Finnzymes Oy, Espoo, Finland). A clone library was constructed using the pGEM-T Easy Vector System I (Promega Corporation, Madison, WI) and NEB 5- $\alpha$  electrocompetent *E. coli* cells (New England BioLabs, Frankfurt, Germany). Cloned sequences were aligned against the public database NCBI using the BLAST algorithm. Only sequences of the most similar type strains and those of uncultured bacteria from published work were downloaded for further phylogenetic analysis. The 9 sequences of MTB from Lake Pavin, their closest relatives identified by BLAST and several representatives of *Proteobacteria* were aligned using MAFFT (Kato and Standley, 2013), giving an alignment of 1529 bp after removal of ambiguous positions. A maximum-likelihood (ML) phylogenetic tree was built with RAxML 8.2.6 (Stamatakis, 2014) under the GAMMA model of rate heterogeneity using empirical nucleotide frequencies and the GTR substitution model. A total of 349 bootstrap replicates automatically determined by the MRE-based bootstrapping criterion were conducted under the rapid bootstrapping algorithm, among which 100 were sampled to generate proportional support values (those under 70 were not shown). Two sequences were affiliated to the same species if aligned sequences shared more than 99 % similarity.

### Synchrotron-based x-ray microfluorescence and scanning electron microscopy analyses

For correlative x-ray microfluorescence and SEM analyses, 100 mL of water collected at the oxic-anoxic interface were filtered on a 0.22 µm polycarbonate filter in a glovebag under N<sub>2</sub>. Micro x-ray fluorescence ( $\mu$ -XRF) experiments were performed on the LUCIA beamline at SOLEIL synchrotron. Measurements were performed at room temperature, under vacuum (10<sup>-2</sup> mbar), using an incident beam at 2500 eV with 4\*4 µm steps and 2 s counting time. All measurements were performed by collecting the fluorescence signal, using a Silicon Drift Detector (SDD). All samples were analysed with their surface perpendicular to the incident beam and grazing incidence with the SDD. This geometry is optimised to minimise self-absorption

effects. Thus, no self-absorption correction was applied. The *per* pixel x-ray fluorescence spectra were corrected for background using a polynomial baseline approximation and fitted to a Gaussian peak shape model with the programme PyMCA (Solé *et al.*, 2007) (batch fit procedure). The fitted P K lines were used to draw the fluorescence intensity map of phosphorus. The resulting 508\*672 µm map allowed determination of the spatial distribution of the major P hotspots on the polycarbonate filter. More details on the LUCIA beamline can be found in Vantelon *et al.* (2016).

Polycarbonate filters were subsequently carbon coated and P hotspots as detected by  $\mu$ -XRF were systematically analysed by scanning electron microscopy (SEM). SEM analyses were performed using a Zeiss ultra 55 field emission gun SEM. Backscattered electron (BSE) images were acquired using an angle selective backscattered (AsB) detector at an accelerating voltage of 10 kV and a working distance of ~7.5 mm. The elemental composition of mineral phases was determined by energy dispersive x-ray spectrometry (EDXS) using an EDS QUANTAX detector. EDXS data were analyzed using the ESPRIT software package (Bruker).

### Supplementary Information References

- EDER, S.H.K., GIGLER, A.M., HANZLIK, M., WINKLHOFFER, M. (2014) Sub-Micrometer-Scale Mapping of Magnetite Crystals and Sulfur Globules in Magnetotactic Bacteria Using Confocal Raman Micro-Spectrometry. *Plos One* 9, e107356.
- KATO, K., STANDLEY, D.M. (2013) MAFFT multiple sequence alignment software version 7: improvements in performance and usability. *Molecular Biology and Evolution* 30, 772–780.
- LI, J., MARGARET-OLIVER, I., CAM, N., BOUDIER, T., BLONDEAU, M., LEROY, E., COSMIDIS, J., SKOURI-PANET, F., GUIGNER, J.M., FÉRARD, C., POINSOT, M., MOREIRA, D., LOPEZ-GARCIA, P., CASSIER-CHAUVAT, C., CHAUVAT, F., BENZERARA, K. (2016) Biomineralization patterns of intracellular carbonatogenesis in cyanobacteria: Molecular hypotheses. *Minerals* 6, #10.
- SCHÜLER, D. (2002) The biomineralization of magnetosomes in *Magnetospirillum gryphiswaldense*. *International Microbiology* 5, 209–214.
- SOLÉ, V.A., PAPIILLON, E., COTTE, M., WALTER, P., SUSINI, J. (2007) A multiplatform code for the analysis of energy-dispersive X-ray fluorescence spectra. *Spectrochimica Acta Part B* 62, 63–68.
- STAMATAKIS, A. (2014) RAxML version 8: a tool for phylogenetic analysis and post-analysis of large phylogenies. *Bioinformatics* 30, 1312–1313.
- TIJSSSEN, J.P.F., BEEKES, H.W., VANSTEVENINCK, J. (1982) Localization of polyphosphates in *Saccharomyces fragilis*, as revealed by 4,6-Diamidino-2-Phenylindole fluorescence. *Biochimica et Biophysica Acta* 721, 394–398.
- VANTELON, D., TRCERA, N., ROY, D., MORENO, T., MAILLY, D., GUILLET, S., METCHALOV, E., DELMOTTE, F., LASSALLE, B., LAGARDE, P., FLANK, A.-M. (2016) The LUCIA beamline at SOLEIL. *Journal of Synchrotron Radiation* 23, 635–640.
- WOLFE, R.S., THAUER, R.K., PFENNIG, N. (1987) A “capillary racetrack” method for isolation of magnetotactic bacteria. *FEMS Microbiology Letters* 45, 31–35.

